



PROCESS SYSTEMS INTERNATIONAL, INC.

20 Walkup Drive, Westborough, MA 01581

August 15, 1996
V049-PL-272

Fax No.: (818) 304-9834

Mr. Alan Sibley c/o Ms. Linda Turner
CALIFORNIA INSTITUTE OF TECHNOLOGY
LIGO Project
102-33 East Bridge Laboratory
Pasadena, CA 91125

Subject: **CAA Report and Technical Article**

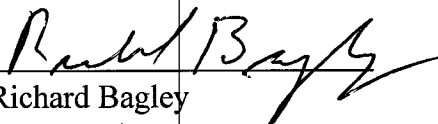
Dear Alan:

Enclosed please find a copy of Cambridge Acoustical Associates (CAA) preliminary report on 80K pump bubble noise.

Also enclosed is a technical paper CAA has requested permission to publish. Please review and respond A.S.A.P.

Please call if you have any questions.

Sincerely,


Richard Bagley
LIGO Project Manager

REB/lml

cc: John Worden - WA Site
LIGO File

CAMBRIDGE ACOUSTICAL ASSOCIATES, INC.

CONSULTING IN ACOUSTICS • NOISE & VIBRATION • STRUCTURAL & FLUID DYNAMICS

200 Boston Avenue, Suite 2500

Medford, MA 02155-4243

Telephone (617) 396-1421

Fax (617) 396-1607

12 September 1996

Process System International, Inc.
20 Walkup Drive
Westborough, Ma 01581

Reference: PSI P.O. # 554386-00

Attn.: Richard Bagley

Enclosed is a copy of a paper entitled "Buoyancy-Propelled Bubble Migration" by Miguel Junger of CAA. With the permission of PSI/LIGO he would like to publish it in the Journal of Acoustic Society of America. Please acknowledge. Also enclosed is a copy of Miguel Junger's report to PSI entitled "Bubble-Generated Forces and Resulting Structure-borne Noise".

Sincerely



Kyle Martini

Buoyancy-propelled bubble migration

Miguel C. Junger
Cambridge Acoustical Associates, Inc.
200 Boston Avenue, Suite 2500
Medford, MA 02155-4243

(Received

Abstract

This paper is intended to supplement the extensive literature on the acoustics of bubble pulsations and on sound propagation in bubble swarms. The vertical migration of bubbles is formulated explicitly using Stokes's formula for low Reynolds number viscous drag. For a sphere, the ratio of displaced liquid mass is twice the entrained mass. The initial bubble size-independent acceleration is therefore $2g$. The ratio of these two masses being larger for slender buoyant bodies whose axis is vertical, their acceleration is even higher. The late time velocity, controlled by viscous drag, tends to an asymptotic value proportional to the bubble's surface area.

Pacs numbers: 43.30.Es, 43.30.Jx, 43.30.Ky, 43.30.Ft

INTRODUCTION

The effect of bubble swarms on sound propagation as well as the sound field radiated by bubble pulsations has been extensively studied. An exhaustive, up-to-date

Miguel C. Junger, J. Acoust. Soc. Am.

bibliography is found in Feuillade's paper.¹ This author is, however, unaware of any explicit formulation of the vertical migration of bubbles, though differential equations describing the dynamics of translating bubbles or bubbles in a flowing liquid are available, e.g., in Leighton's recent monograph.² In this paper, a simple expression is derived for the low Reynolds number migration of a buoyancy driven bubble. This solution can be combined with the above mentioned familiar analysis of bubble pulsations, thereby describing the acoustics of buoyancy-propelled bubbles. For the present purpose, the bubble is modelled as a sphere of negligible mass.

I. EQUATIONS OF MOTION

The bubble's upwards motion is driven by its buoyancy, viz. by the weight of displaced liquid:

$$F_b = \rho Vg \quad (1)$$

where

ρ = *liquid density*

V = *bubble volume* = $4\pi a^3/3$

a = *bubble radius*

g = *acceleration of gravity*

The bubble's motion is resisted by the inertia force F_i of the entrained mass which, for a translating sphere, equals half the displaced mass³:

Miguel C. Junger, J. Acoust. Soc. Am.

$$F_i = \rho V \ddot{U} / 2 \quad (2)$$

where \ddot{U} = bubble acceleration. A third force is the drag F_d . For bubbles starting from rest, the Reynolds number is low, there being no wake at the bubble's rear. The drag will be approximated by Stokes's expression⁴:

$$F_d = 6\pi \nu \rho a \dot{U} \quad (3)$$

where ν is the kinematic viscosity in units of length squared/time. This expression is strictly valid for a sphere moving at constant velocity. This approximation is selected because the resulting simple solution provides ready insight to the physics of bubble dynamics. The error is negligible at early times, where viscous drag is overshadowed by the inertia force, and at late times, where the velocity has approached its asymptotic constant value \dot{U}_T .

Applying Newton's second law, viz. setting the buoyancy force F_b equal to the sum of the liquid-generated forces, F_i and F_d , one obtains the equation of motion:

$$\frac{1}{2} \rho V \ddot{U} + 6\pi \nu \rho a \dot{U} - \rho V g = 0 \quad (4a)$$

Dividing all terms by $\rho V / 2 = (2\rho \pi a^3 / 3)$,

$$\ddot{U} + \frac{9\nu}{a^2} \dot{U} - 2g = 0 \quad (4b)$$

Once again sacrificing rigor to simplicity, the depth dependence of the bubble radius will

be ignored. The resulting error is insignificant at early times, where inertia predominates over drag. Even at late times, the error is unimportant at shallow depth where the hydrostatic pressure, and consequently bubble size is dominated by atmospheric pressure, and relatively independent of depth, i.e., of the vertical distance U migrated by the bubble.

II. BUBBLE MIGRATION

Assuming that the bubble starts from rest, the resistive term is negligible at early times. For a bubble migration initiated at time zero,

$$\left. \begin{aligned} \ddot{U} &\sim 2g \\ \dot{U} &\sim 2gt \\ U &\sim gt^2 \end{aligned} \right\} t \ll \frac{a^2}{9\nu} \quad (5)$$

The large acceleration is due to the fact that the entrained mass is half the displaced mass of liquid³. It is independent of bubble size, but is a function of the buoyant body's aspect ratio: A slender body, viz. a vertically oriented prolate spheroid, experiences even larger acceleration, its entrained mass being a smaller fraction of the displaced mass.

At late times, viscous drag overshadows the inertia force. Equating buoyancy to drag one solves for the asymptotic terminal velocity

$$\dot{U} \sim \dot{U}_T \equiv 2ga^2/9\nu, \quad t \gg a^2/9\nu \quad (6)$$

The equation of motion, Eq. 4b, is conveniently formulated in terms of this asymptotic velocity:

$$\ddot{U} + \frac{2g}{\dot{U}_T} \dot{U} - 2g = 0 \quad (7)$$

The solution of this differential equation is

$$\dot{U}(t) = \dot{U}_T [1 - \exp(-2gt/\dot{U}_T)] \quad (8a)$$

Differentiating, the acceleration is

$$\ddot{U}(t) = 2g \exp(-2gt/\dot{U}_T) \quad (8b)$$

Integrating Eq. 8a, the displacement is

$$U(t) = \dot{U}_T t - (\dot{U}_T^2/2g)[1 - \exp(-2gt/\dot{U}_T)] \quad (8c)$$

Eqs. 8 are plotted in Fig. 1 for two bubble sizes, the liquid being water ($\nu \approx 10^{-2} \text{ cm}^2/\text{s}$ at room temperature). While the asymptotic terminal velocity \dot{U}_T increases with bubble size, early time dynamics are independent of bubble dimensions. This trend, as well as the associated slower attenuation of the acceleration \ddot{U} of the larger bubble are illustrated in the graphs.

ACKNOWLEDGEMENT

Numerical results were generated by the author's coworker, Jason Rudzinsky. The permission to publish this study was graciously extended by PSI, the company which sponsored this work in connection with the development of laser interferometer equipment designed to observe gravitational waves.

Bibliography

- 1 C. Feuillade, "Attenuation and dispersion of sound in water containing multiple interacting air bubbles", J. Acoust. Soc. Am. 99, 3412-3430 (June 1996).
Miguel C. Junger, J. Acoust. Soc. Am.

- 2 T.G. Leighton, The Acoustic Bubble, (Academic Press, London, 1994), "The translating bubble", pp. 113 et seq.
- 3 H. Lamb, Hydrodynamics, 6th ed. (Dover, New York, 1945), p. 124, Eq. 3.
- 4 Ibid, p. 598, Eq. 15.

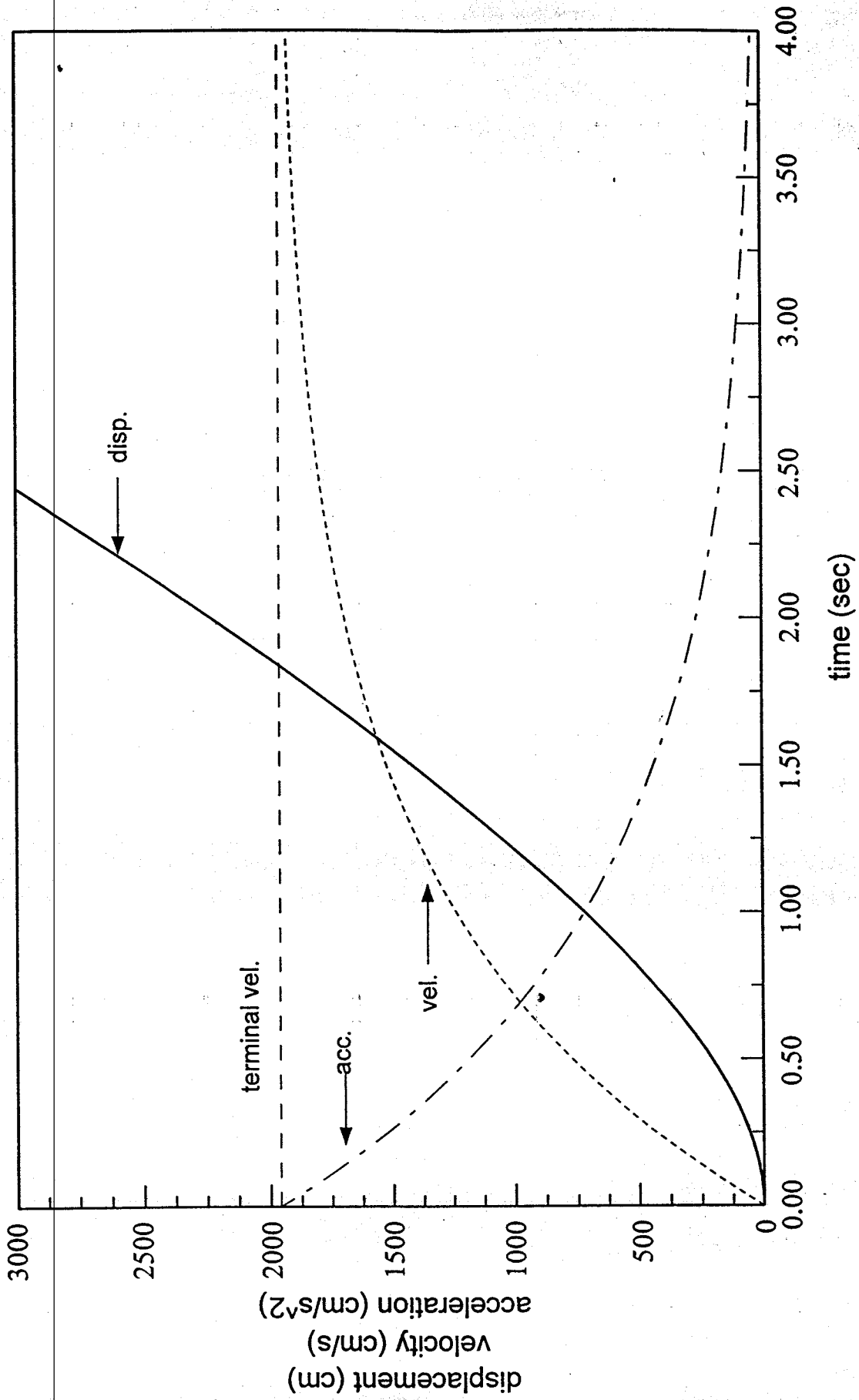
Figure Captions

Fig. 1 Acceleration, velocity, and displacement of buoyancy-propelled bubbles.

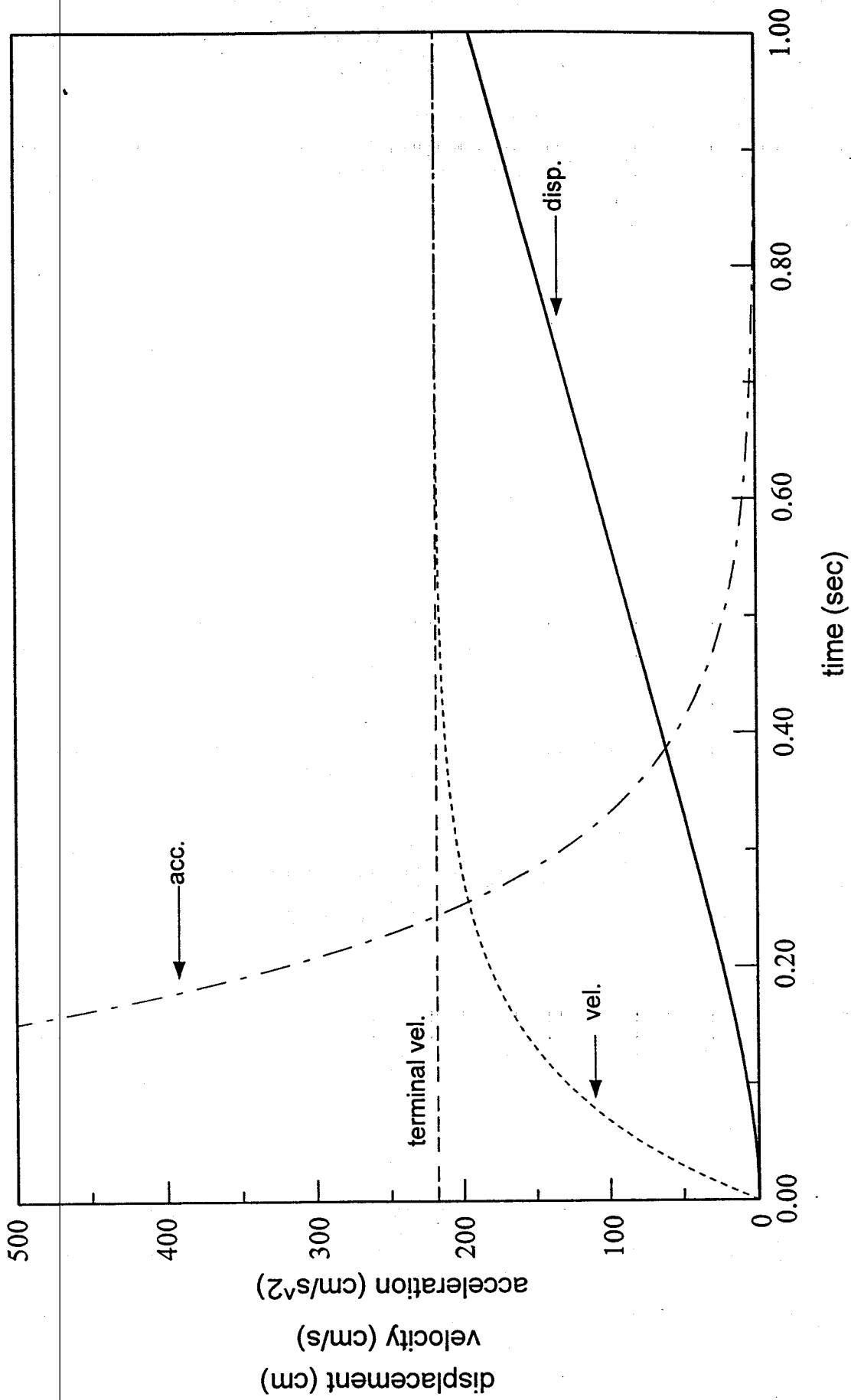
Fig. 1(a): Bubble radius 0.1 cm.

Fig. 1(b): Bubble radius 0.3 cm.

Unimpeded Bubble Rise in Water ($a=0.3$ cm)



Unimpeded Bubble Rise in Water ($a=0.1$ cm)



CAMBRIDGE ACOUSTICAL ASSOCIATES, INC.

CONSULTING IN ACOUSTICS • NOISE & VIBRATION • STRUCTURAL & FLUID DYNAMICS

200 Boston Avenue, Suite 2500

Medford, MA 02155-4243

Telephone (617) 396-1421

Fax (617) 396-1607

TO: Richard Bagley, PSI

FROM: M.C. Junger

DATE: 26 August 1996

SUBJECT: BUBBLE-GENERATED FORCES AND RESULTING
STRUCTURE-BORNE NOISE

TECH MEMO: TM/U-2392-2041

ABSTRACT

The dynamics of vapor bubbles in the boiling liquid nitrogen between the two concentric cylindrical tanks and the resulting force spectrum exerted on the outer tank are formulated. Finally, the resulting acceleration spectrum level of the outer tank wall is computed.

I. BUBBLE DYNAMICS

Heat transfer across the outer tank surfaces causes the liquid nitrogen to boil. The resulting vapor bubbles rise vertically with a velocity $\dot{U}(t)$ until they collide with the surface of the inner or outer tank (Fig. 1). This analysis deals with the structure-borne noise generated by the bubbles colliding with the outer tank wall. The strongest impact force is exerted by bubbles emerging from the greatest vertical path length d , viz. a path not resulting in grazing along the inner tank wall.

A rising bubble is subjected to three forces: The buoyancy B , the inertial force $M\ddot{U}$ of the entrained mass of water, and drag $D\dot{U}$ associated with the liquid's viscosity. For the present parameter values, drag is by far the smallest of the three forces. It will be approximated by Stokes's simple expression for low-Reynolds numbers. The drag coefficient¹ is

$$D = 6\pi\nu\rho a \quad (I.1a)$$

where ν = kinematic viscosity = $1.9 \times 10^{-3} \text{cm}^2/\text{s}$ for liquid nitrogen,
as compared to $10^{-2} \text{cm}^2/\text{s}$ for water at room temperature

$$\rho = \text{density} = 0.81 \text{g/cm}^3$$

$$a = \text{mean bubble radius} = 3/64 \text{in.} = 0.12 \text{cm}$$

Consequently,

$$D = 3.48 \times 10^{-3} \text{dyne} \cdot \text{s/cm} \quad (\text{I.1b})$$

Though this expression was derived for constant flow velocity, it provides a good approximation, as drag only becomes predominant when the bubble velocity has approached its asymptotic value [Eq. I.6a below].

The mass is the entrained mass of a translating sphere small in terms of wavelengths, viz. half the displaced mass of liquid²:

$$\begin{aligned} M &= 2\pi a^3 \rho / 3 \\ &= 2.93 \times 10^{-3} \text{grams} \end{aligned} \quad (\text{I.2})$$

The error resulting from the assumed constant bubble volume is small, because hydroacoustic pressure at shallow depth is primarily a function of the gas pressure on the liquid surface rather than of depth. The buoyant force is the weight of displaced liquid:

$$B = \frac{4\pi a^3 \rho g}{3} \quad (\text{I.3a})$$

where g is the acceleration of gravity, viz. 980cm/s^2 . Consequently,

$$B = 7.09 \text{ dynes} \quad (\text{I.3b})$$

The equation of motion therefore becomes

$$M\ddot{U} + D\dot{U} - B = 0, \quad 0 < t < t_0 \quad (I.4)$$

It is convenient to divide this equation by M and to express the ratios D/M and B/M explicitly:

$$\ddot{U} + \frac{9\nu}{a^2} \dot{U} - 2g = 0 \quad (I.5a)$$

At early times, the bubble rises at twice the acceleration of gravity, irrespective of its volume:

$$\left. \begin{aligned} \ddot{U} &\approx 2g \\ \dot{U} &\approx 2gt \\ &= 1960t \end{aligned} \right\} \begin{aligned} (9\nu/a^2) \dot{U} &\ll 2g \\ t &\ll \frac{a^2}{9\nu} = 0.84s \end{aligned} \quad (I.5b)$$

At late times, when drag predominates over the inertia force, the bubble velocity tends asymptotically to

$$\begin{aligned} \dot{U}_T &\approx \frac{2a^2g}{9\nu}, \quad t \gg \frac{a^2}{9\nu} \\ &= 1.65 \times 10^3 \text{ cm/s} = 59.4 \text{ km/hr} \end{aligned} \quad (I.6a)$$

The solution of Eq. 1.5a is (Figs. 2a and b)

$$\dot{U} = \dot{U}_T \left[1 - \exp\left(-\frac{2gt}{\dot{U}_T}\right) \right]$$

$$\ddot{U} = 2g \exp(-2gt/\dot{U}_T) \quad (I.6b)$$

$$U(t) = \int_0^t \dot{U} dt$$

$$= \dot{U}_T t - \frac{\dot{U}_T^2}{2g} \left[1 - \exp\left(-\frac{2gt}{\dot{U}_T}\right) \right] \quad (I.6c)$$

For the maximum unimpeded vertical path of a rising bubble, viz.

$U = d = 68.6m$, the terminal velocity and acceleration are

$$\left. \begin{aligned} \dot{U}(t_o) &= 500 \text{ cm/s} = 18 \text{ km/hr} \\ \ddot{U}(t_o) &= 1.41 \times 10^3 \text{ cm/s}^2 \\ &= 1.44g \end{aligned} \right\} t_o = 0.279s \quad (I.7a)$$

Since the drag is relatively small, approximate values of rise time and velocity are

$$\left. \begin{aligned} t_o &\approx (d/g)^{1/2} = 0.26s \\ \dot{U}(t_o) &\approx 2(dg)^{1/2} = 518 \text{ cm/s} \end{aligned} \right\} D\dot{U} \ll M\ddot{U} \quad (I.7b)$$

II. SPECTRUM LEVEL OF THE IMPACT FORCE EXERTED BY A BUBBLE ON THE OUTER SHELL

The bubble colliding with the outer shell exerts a time dependent vertical force

$$\left. \begin{aligned} F &= M\ddot{u}_D(t) \\ &= M\ddot{U}_D \Phi(t), \quad 0 < \phi(t) < 1 \end{aligned} \right\} 0 < t < \tau \quad (II.1)$$

where M is once again the entrained mass of liquid attached to the rising bubble (Eq. I.2)

and \ddot{u}_D is the bubble's deceleration sensed by the bubble during a time interval τ . In the absence of data or of a detailed analysis, it will be assumed that the deceleration takes place in a time interval equal to the time in which the bubble rises through a distance equal to its diameter:

$$\begin{aligned}\tau &= \frac{2a}{\dot{U}(t_o)} \\ &= \frac{0.24 \text{ cm}}{500 \text{ cm/s}} = 4.8 \times 10^{-4} \text{ s}\end{aligned}\tag{II.2}$$

where $\dot{U}(t_o)$ is the terminal bubble velocity where it reaches the shell surface (Eq. 1.7a). This velocity is cancelled as the bubble is brought to a halt. In the absence of detailed information on this process and in view of the primary interest in the low frequency portion of the spectrum where the time history is relatively unimportant, it will be assumed that the deceleration displays a semi-sinusoidal time dependence:

$$\Phi(t) = \sin\left(\frac{\pi t}{\tau}\right), \quad 0 \leq t \leq \tau\tag{II.3}$$

The bubble comes to a halt when

$$\begin{aligned}\dot{U}(t_o) &= \ddot{U}_D \int_0^{\tau} \sin\left(\frac{\pi t}{\tau}\right) dt \\ &= \frac{2\tau}{\pi} \ddot{U}_D\end{aligned}\tag{II.4}$$

Solving for the deceleration amplitude,

$$\ddot{U}_D = \frac{\pi \dot{U}(t_0)}{2\tau} \quad (\text{II.5a})$$

$$= \frac{\pi \dot{U}^2(t_0)}{4a} \quad (\text{II.5b})$$

$$= 1.64 \times 10^6 \text{ cm/s}^2$$

The force exerted by the bubble can now be expressed explicitly by substituting Eqs. I.2 and II.5b in Eq. II.1:

$$F(t) = \frac{\rho [\pi a \dot{U}(t_0)]^2}{6} \sin\left(\frac{\pi t}{\tau}\right), \quad 0 \leq t \leq \tau \quad (\text{II.6})$$

This is plotted in Figs. 3a and b.

The Fourier transform of the normalized deceleration history is³

$$\begin{aligned} \tilde{\phi}(\omega) &= \int_0^{\tau} \sin\frac{\pi t}{\tau} e^{i\omega t} dt \\ &= \frac{\pi\tau(1 + e^{i\omega\tau})}{\pi^2 - \omega^2\tau^2} \\ &= \frac{2\pi\tau \cos(\omega\tau/2)}{\pi^2 - \omega^2\tau^2} e^{i\omega\tau/2} \end{aligned} \quad (\text{II.7})$$

whose absolute value is

$$\begin{aligned}
 |\tilde{\phi}(\omega)| &= \frac{2\pi\tau |\cos(\omega\tau/2)|}{|\pi^2 - \omega^2\tau^2|} \\
 &\approx \frac{2\tau}{\pi} \left. \begin{array}{l} \\ \\ \end{array} \right\} \begin{array}{l} (\frac{\omega\tau}{\pi})^2 \ll 1 \\ (f/Hz)^2 \ll (4 \times 10^3)^2 \end{array} \quad (II.8) \\
 &= 3.1 \times 10^{-4} s
 \end{aligned}$$

The force spectrum can now be computed. It is first noted that the radial force is (Fig. 1)

$$\begin{aligned}
 F_R &= F \sin \phi_o \\
 &= F d / 2R_o \\
 &= 0.45 F \quad (II.9)
 \end{aligned}$$

Combining Eqs. I.2, II.1,2, 8 and 9, the spectrum of the radial force is formulated explicitly:

$$|\tilde{F}_R(\omega)| = \frac{M\dot{U}(t_o)d}{2R_o}, \quad \omega^2\tau^2 \ll \pi^2 \quad (II.10a)$$

Substituting the parameter values,

$$\begin{aligned}
 |\tilde{F}_R(\omega)| &= 0.66 \text{ dyne}\cdot\text{s}, \quad f^2 \ll (4 \times 10^3 \text{ Hz})^2 \\
 20 \log |\tilde{F}_R(\omega)| &= -3.6 \text{ dB re}(\text{dyne}\cdot\text{s})^2 \quad (2.10b)
 \end{aligned}$$

It is recalled that selecting the terminal velocity $\dot{U}(t_o)$ corresponding to a bubble rising from the maximum depth avoiding grazing the inner tank is one more conservative

assumption.

III. ACCELERATION SPECTRUM LEVEL OF THE OUTER SHELL

The radial drive-point velocity \dot{w} of a cylindrical shell driven by a radial harmonic force is formulated in terms of the shell's admittance:

$$Y_c(\omega) \equiv \frac{\dot{w}(\omega)}{\tilde{F}_R(\omega)} \quad (\text{III.1a})$$

corresponding to the radial acceleration

$$|\ddot{w}(\omega)| = \omega |Y_c(\omega) \tilde{F}_R(\omega)| \quad (\text{III.1b})$$

Y_c is the series of modal admittances which peak at the lower natural frequencies of the predominantly radial family of the three families of modes of a cylindrical shell. These resonances, identified by the circumferential wavenumber n/R_o , are in the mid-frequency range (Ref. 4, p. 225, Fig. 7.6; $1 \leq n \leq 5$). Since even the approximate calculation of the admittance is laborious (Ref. 4, p. 226-227, Eqs. 7.99 and 7.101), an estimate of the shell acceleration will be based on the admittance vs. frequency graph in Ref. 4, p. 228, Fig. 7.7 reproduced in this report as Fig. 4. This graph is for a shell of thickness-to-radius ratio $h/R_o = 10^{-2}$ and an aspect ratio $L/2R_o = 2$, both of which fall close to the corresponding values of the present shell for which $h/R = 1.34 \cdot 10^{-2}$ and $L/2R_o = 2.45$. A possibly more serious discrepancy arises from the fact that Fig. 4 corresponds to simply supported boundary conditions, and to a midspan drive-point, $x_o = L/2$. For this situation, even modes are associated with their maximum generalized force, while the odd modes are not excited. These two effects partially cancel for randomly applied forces.

A major highly conservative approximation is the neglect of the radiation loading

exerted by the liquid-filled annular space between the concentric shells. Unless the structure-borne noise spectrum level predicted by this simple analysis exceeds the specifications, there is no incentive to perform a more rigorous study.

In this low-frequency range, the admittance in Fig. 4 is described by the equation

$$20 \log |Y_c/Y_p| = 15 \text{ dB} + 20 \log \Omega, \quad \Omega \leq 0.03 \quad (\text{III.2})$$

where the dimensionless frequency formulated in terms of the dilatational plate velocity c_p ($= 5.4 \times 10^5 \text{ cm/s}$ for steel and aluminum) is

$$\begin{aligned} \Omega &\equiv \omega R_o / c_p \\ &= 8.80 \times 10^{-4} f / \text{Hz} \end{aligned} \quad (\text{III.3})$$

Y_p is the admittance of an infinite plate of the same material and thickness as the shell⁵:

$$Y_p = 3^{1/2} / 4 \rho_s c_p h^2 \quad (\text{III.4})$$

where ρ_s is the density of the plate material ($= 2.8 \text{ g/cm}^3$ for aluminum), and where the plate thickness $h = 3/8 \text{ in.} = 0.95 \text{ cm}$. Substituting these parameter values, one obtains

$$\begin{aligned} 20 \log Y_p &= 20 \log [3.16 \times 10^{-7} (\text{cm/s}) / \text{dyne}] \\ &= -130.0 \text{ dB re } (\text{cm/s} \cdot \text{dyne})^2 \end{aligned} \quad (\text{III.5})$$

The shell admittance level corresponding to Eq. III.2 finally becomes

$$\begin{aligned} 20 \log |Y_c| \text{ dB re } (\text{cm/s} \cdot \text{dyne})^2 &= -176 \text{ dB} \\ &+ 20 \log (f / \text{Hz}), \quad f \leq 30 \text{ Hz} \end{aligned} \quad (\text{III.6})$$

In the low-frequency range, the simply supported shell can therefore be modelled as a

spring of stiffness

$$\begin{aligned} K &= \frac{\omega}{|Y_c|} \\ &= 4.0 \times 10^9 \text{ dyne/cm} \end{aligned} \quad (\text{III.7})$$

It is noted that Eq. III.6 is not conservative in the resonance frequency range $30 \text{ Hz} < f < 80 \text{ Hz}$, where the error does not however exceed 7 dB for the assumed structural loss factor of $\eta_s = 0.1$. The resonance response is evaluated in the last paragraph of this section. Eq. III.6 is highly conservative at higher frequencies.

The tank's acceleration spectrum level can now be formulated in terms of the convolution theorem⁶. From Eq. III.1b the spectrum level generated by N bubbles per second colliding with the tank is

$$L_{acc} \text{ dB re } (cm/s^2)^2/Hz = 20 \log [2\pi \omega |\tilde{F}_R(\omega) Y_c(\omega)|] + 10 \log N \quad (\text{III.8})$$

Noting that

$$20 \log (2\pi \omega) = 31.9 \text{ dB} + 20 \log (f/Hz) \quad (\text{III.9})$$

Substituting the numerical values from Eqs. II.10b and III.9 in Eq. III.8, the low-frequency acceleration spectrum level becomes

$$\left. \begin{aligned} L_{acc} &= -148 \text{ dB re } [(cm/s^2)^2/Hz] \\ &= -88 \text{ dB re } [(\mu g)^2/Hz] \end{aligned} \right\} + \log f + 10 \log N \quad (\text{III.10a})$$

$$= +15 \text{ dB re } [(\mu g)^2/Hz], f = 30 \text{ Hz}, N = 26,000s^{-1} \quad (\text{III.10b})$$

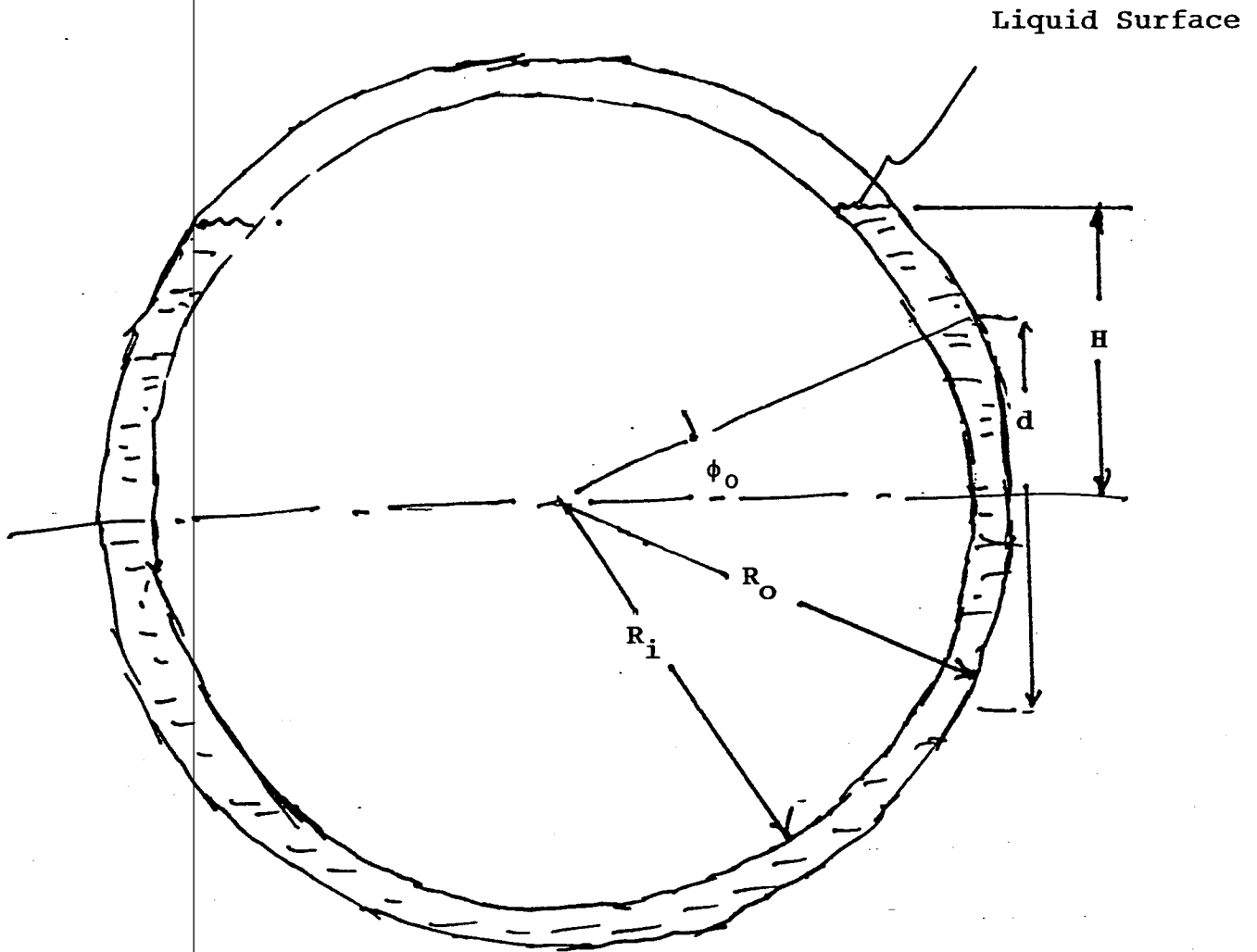
The peak value is associated with the resonance peak in Fig. 4 at $\Omega = 0.058$, $f = 66 \text{ Hz}$, where Eq. III.6 is approximately 7 dB too low. The highest spectrum level is

therefore obtained by substituting $f = 66 \text{ Hz}$ in Eq. III.10a and raising the result by 7 dB. This results in a resonance acceleration spectrum level of $36 \text{ dB re } [(\mu\text{g})^2/\text{Hz}]$. The corresponding displacement spectrum level is obtained by subtracting $40 \log dB(2\pi f) = 104 \text{ dB}$, resulting in a resonance displacement spectrum level of $-128 \text{ dB re cm}^2/\text{Hz}$.

Acknowledgement: Numerical results in Figs. 2 and 3 were generated by the author's coworker Jason Rudzinsky.

REFERENCES

- 1 H. Lamb, Hydrodynamics, 6th ed. (Dover, 1945), p; 598, EQ. 15.
- 2 Ibid., p. 124, Eq. 3.
- 3 B.O. Peirce, A Short Table of Integrals, 3rd ed. (Ginn, Boston 1929), p. 54, integral 414, with $a = i\omega..$
- 4 M.C. Junger and D. Feit, Sound, Structures, and Their Interaction, 2nd. ed. (MIT Press 1986, reprinted by Amer. Inst. of Physics 1993), p. 225-228.
- 5 Ibid., p. 212, Eq. 7.68.
- 6 A. Papoulis, The Fourier Integral and Its Applications, (Mc Graw-Hill, New York, 1962), pp. 26-28.



$$R_o = 29 \frac{3}{4} \text{ in.} = 75.6 \text{ cm}$$

$$R_i = 26 \frac{1}{2} \text{ in.} = 67.3 \text{ cm}$$

$$H = 21 \text{ in.} = 53.3 \text{ cm}$$

$$d = 2[R_o^2 - R_i^2]^{1/2} = 27 \text{ in.} = 68.7 \text{ cm}$$

$$\phi_o = \tan^{-1} d/2R_i = \sin^{-1} d/2R_o = 27^\circ$$

Fig. 1 Configuration of concentric shells.

Unimpeded Bubble rise in liquid nitrogen.

$2a = 0.24 \text{ cm}$

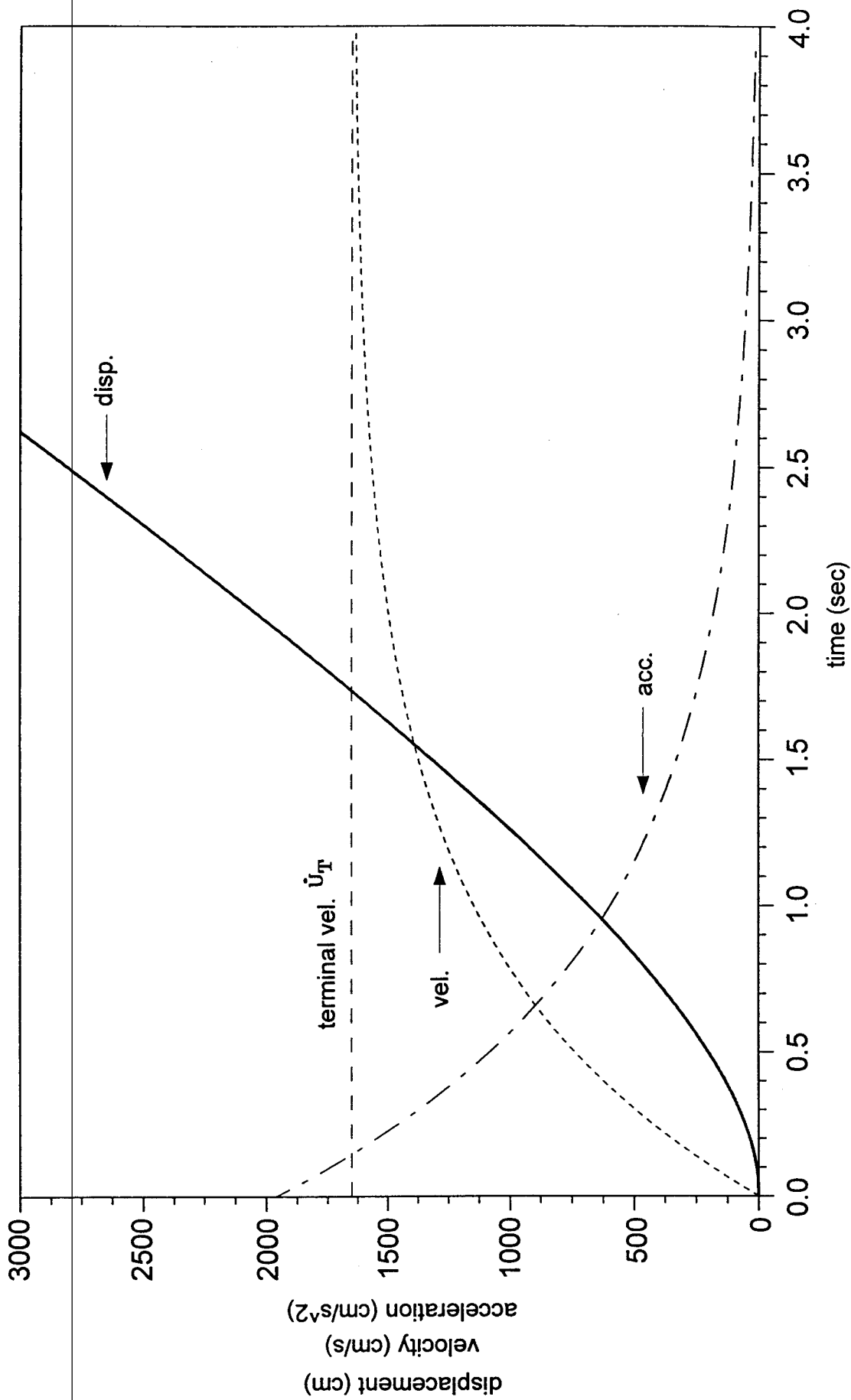


Fig. 2 Acceleration, velocity and vertical displacement of a bubble (Eqs. 1.6b and c).

Fig. 2a Extended time history.

Unimpeded bubble rise in liquid nitrogen.
 $2a = 0.24 \text{ cm}$

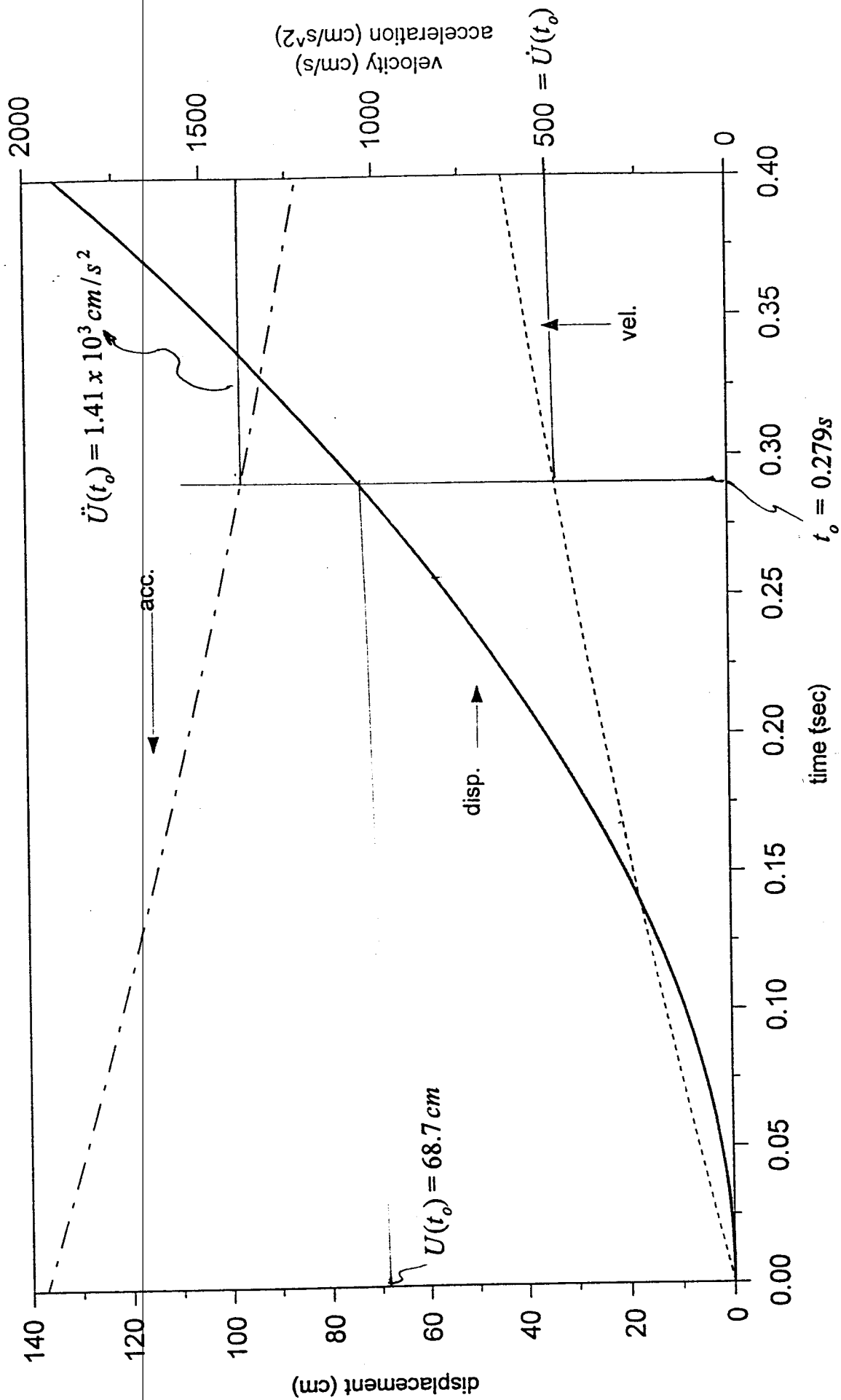


Fig. 2b Early time history relevant to tank dimensions, (Eq. 1.7a).

Unimpeded bubble rise in liquid nitrogen.

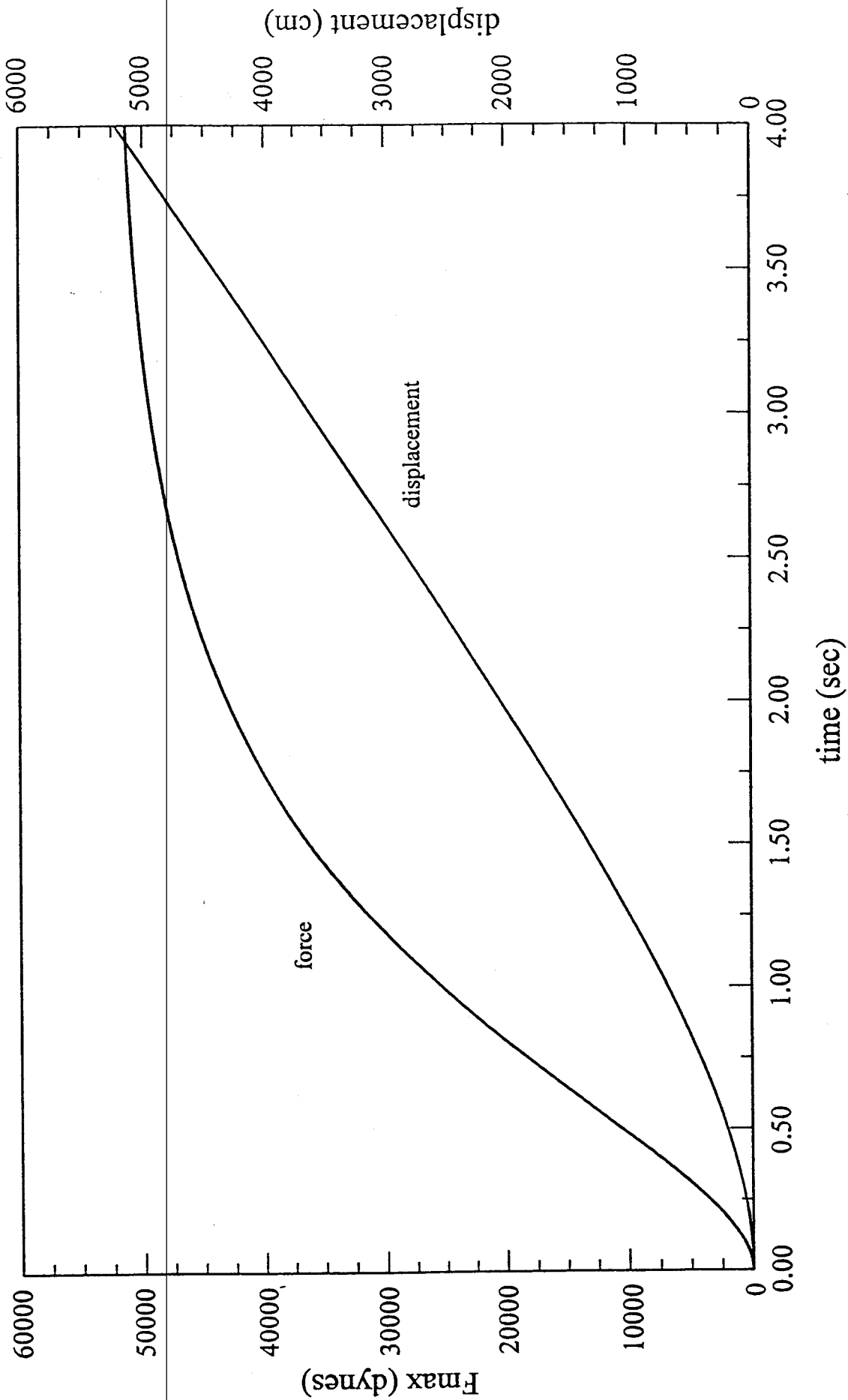


Fig. 3 Vertical force amplitude applied by the bubble colliding with shell as a function of time and of vertical distance travelled (Eq. II.6).

Fig. 3a Extended time history.

Unimpeded bubble rise in liquid nitrogen.

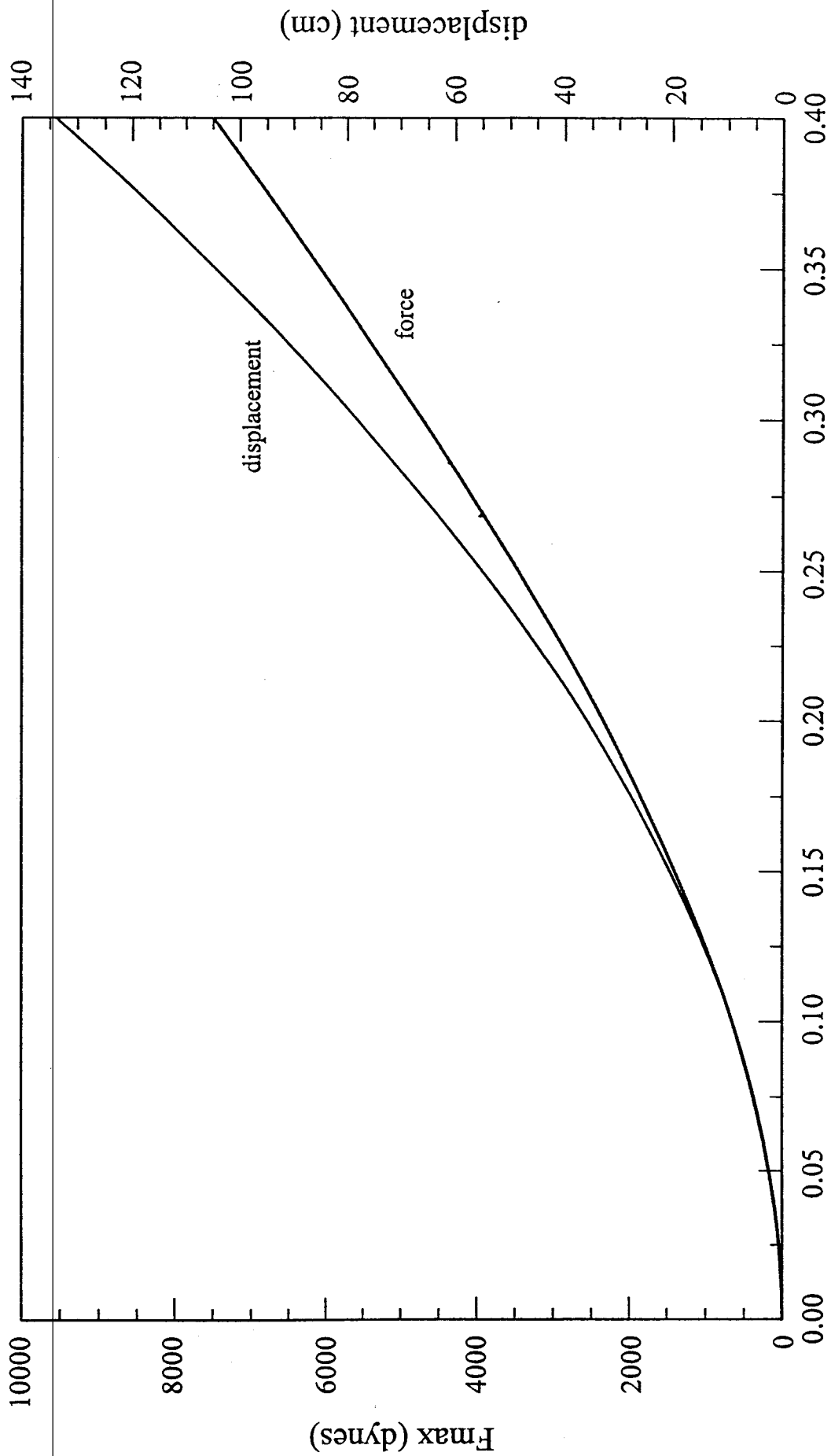


Fig. 3b Early time history relevant to tank dimensions.

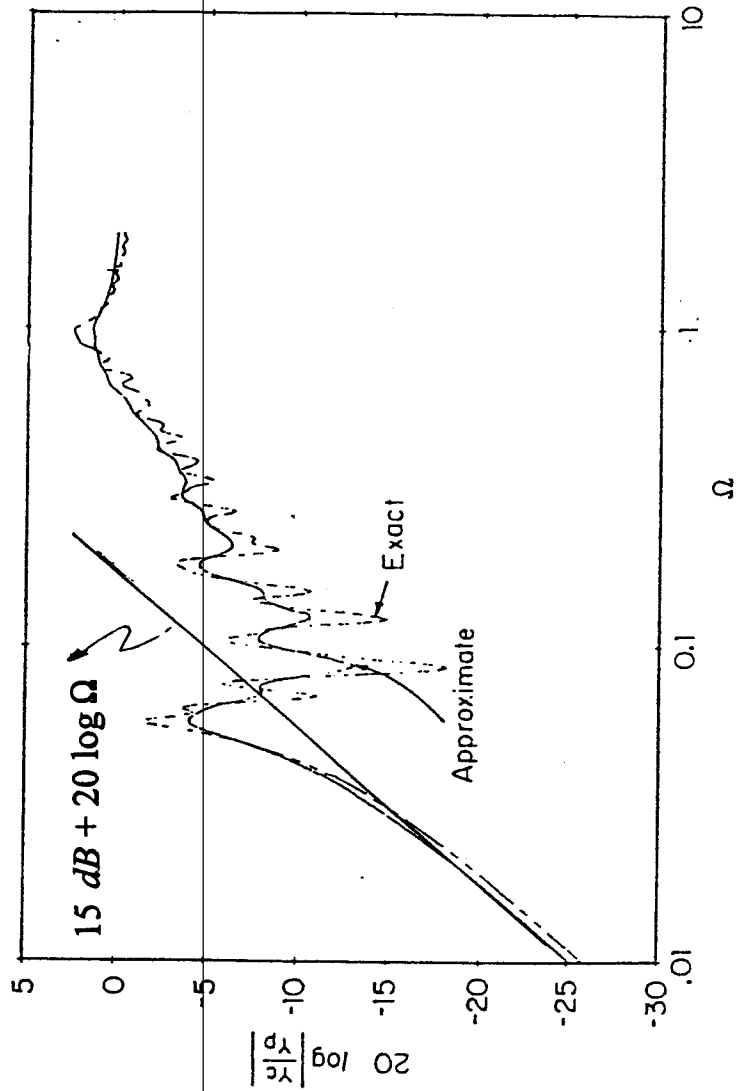


Fig. 4 Admittance of a cylindrical shell [s.s., driven at midspan, $h/a = 10^{-2}$, aspect ratio 2] normalized to the point admittance of an infinite plate of thickness h . (Reproduced from Ref. 4)